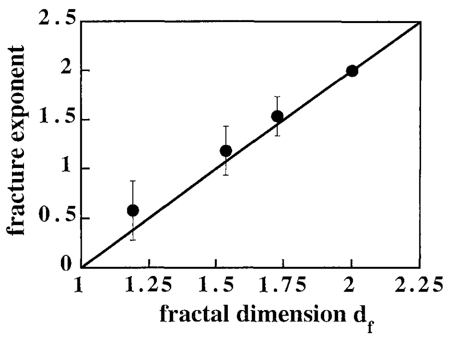

Fig. 5. The absolute value of the measured exponent of activation energy versus force as a function of the fractal dimension of the gels. The point at $d_f = 2$ is the measurement of (*5*) for a two-dimensional crystal. The line is the prediction from the scaling arguments presented in the text.

are visco-elastic and thus have an inherent relaxation time. However, the three different gels have practically the same visco-elastic moduli, in spite of the observed large difference in their fracture behavior. Moreover, as is evident from Fig. 1A, no visco-elastic relaxations were found for low frequencies. These low frequencies equal the inverse of the measured t_b; the important visco-elastic relaxations occur at much higher frequencies, higher by several orders of magnitude. Third, the results for the two-dimensional single crystals also agree with the findings for the gels.

A fracture that propagates very slowly and suddenly becomes unstable, a so-called creep fracture, would be another explanation for our experimental results (*11*). A typical example is a small crack in a windshield; it does not propagate because the crack front is trapped on impurities in the material. In studying the fracture dynamics of the gel with high-speed photography (Fig. 2), we sometimes saw this lattice trapping, but it never lasted longer than a fraction of a second. Thus, the energy barriers involved in lattice trapping are much smaller than the barrier for the nucleation of the initial crack, and it seems unlikely that this mechanism applies. More generally, our results cannot be understood by considering a distribution of preexisting flaws that grow and lead to the failure of the material, because in the three-point flexion geometry of our experiment, the initial crack always starts to propagate opposite to where the force is applied.

We have demonstrated and explained the existence of a delayed fracture in an inhomogeneous soft solid. These results should be relevant for the food industry (*12*), in which polymer gels are widely used. However, they could also have implications for the strength of a larger class of composite materials such as two-phase or polycrystalline materials, the fracture properties of which have only been described phenomenologically (*2*, *13*).

REFERENCES AND NOTES

1. L. B. Freund, *Dynamic Fracture Mechanics* (Cambridge Univ. Press, Cambridge, UK, 1990).
2. M. F. Kanninen and C. H. Popelar, *Advanced Fracture Mechanics* (Clarendon, Oxford, 1985).
3. Agarose type XII, I-a, and III-a (denoted as gels 1, 2, and 3) from Sigma was dissolved at 1 weight % in water (Milli-Q-Plus) at 95°C by stirring. Subsequently, the solution was poured into a mold and left for at least 2 hours at 20°C before use. For the three gels, we found E = 75.2, 46.1, and 50.6 kPa. For $\sigma < 50$ Pa or frequency $f < 10$ Hz, the elastic or storage modulus G' = 22.8, 14.6, and 15.6 kPa, respectively. As expected for a gel, Poisson's ratio ≈ 0.5. The ratio of G' and the viscous or loss modulus G'' (G'/G'') is between 10 and 13 for the three gels. Rheological measurements were performed on a Reologica Stress-Tech rheometer. For the fracture experiments, a rectangular bar (100 mm × 20 mm × 10 mm) rested on a Teflon-coated surface greased with liquid Vaseline oil, with its ends held in place by two aluminium rods. The middle flexion point moved on an air bearing and was coupled to a force transducer. A small amount of plastic deformation was observed for the largest forces; in the experiments, the force was always kept constant. Plastic deformation due to aging was not observed in the experiments.
4. A. A. Griffith, *Philos. Trans. R. Soc. London Ser. A* **221**, 163 (1920).
5. L. Pauchard and J. Meunier, *Phys. Rev. Lett.* **70**, 3565 (1993).
6. Y. Pomeau, *C. R. Acad. Sci. Ser. II* **314**, 553 (1992).
7. M. Manno and M. U. Palma, *Phys. Rev. Lett.* **79**, 4286 (1997).
8. D. Avnir, O. Biham, D. Lidar, O. Malcai, *Science* **279**, 39 (1998).
9. D. A. Weitz, J. S. Huang, M. Y. Lin, J. Sung, *Phys. Rev. Lett.* **54**, 1416 (1985).
10. J. Zarzycki, *J. Non-Cryst. Solids* **100**, 359 (1988).
11. M. Marder, *Phys. Rev. E* **54**, 3442 (1996).
12. A. Bot, R. D. Groot, W. G. M. Agterof, in *Gums and Stabilizers for the Food Industry 8*, G. Phillips, P. Williams, D. Wedlock, Eds. (IRL, Oxford, 1996), pp. 117–126.
13. B. Lawn, *Fracture of Brittle Solids* (Cambridge Univ. Press, Cambridge, UK, 1993).

14. We thank M. Adda-Bedia for helpful discussions and V. Bergeron (Rhone-Poulenc) for the use of the high-speed camera. Laboratoire de Physique Statistique de l'Ecole Normale Supérieure is Unité de Recherche Associée 1306 of the CNRS, associated with Universities Paris 6 and 7.

26 November 1997; accepted 19 February 1998

Thermographic Selection of Effective Catalysts from an Encoded Polymer-Bound Library

Steven J. Taylor and James P. Morken*

A general method is introduced for the rapid and simultaneous evaluation of each member of large encoded catalyst libraries for the ability to catalyze a reaction in solution. The procedure was used to select active catalysts from a library of potential polymer-bound multifunctional catalysts. From ~7000 beads screened (3150 distinct catalysts), 23 beads were selected for catalysis of an acylation reaction. Kinetic experiments indicate that the most strongly selected beads are also the most efficient catalysts.

In the development of new catalysts, many iterations of design and redesign are usually required to increase catalyst activity. Accordingly, many research groups have begun to use combinatorial chemistry (*1*) and solid-phase synthesis (*2*) to rapidly produce large numbers of potential catalysts. Despite recent progress in evaluating the thermodynamics of equilibrium processes involving polymer-bound libraries (*3*), methods for assessing the kinetics of reactions involving polymer-bound reagents have not been available. This circumstance has prevented the analysis of very large libraries (10^4 to 10^6 members), because screening for small-molecule catalysts requires an individual assay for each member of a catalyst library. Here, we report the development of a general single-pot assay for large, encoded polymer bead–bound catalyst libraries, which we used to select active catalysts from ~7000 encoded catalyst beads (3150 different catalysts) prepared through "split and pool" solid-phase synthesis. This method is directly applicable to libraries of larger size.

Most chemical reactions have a measurable heat of reaction ΔH_r°, and thus temperature T has been used to survey the progress of catalytic reactions (*4*). Because all catalysts in a parallel library assay are evaluated under the same reaction conditions, the most active catalyst will cause the largest temperature change ($\Delta T \propto$ turnover frequency $\times\ \Delta H_r^\circ$). Recent advances in two-dimensional real-time infrared (IR) thermography have made spatial resolution of temperature possible through measurement of blackbody radiation. Therefore, IR thermography may be used to simultaneously compare the rate of each reaction, in an array of reactions, by measuring the relative reaction temperatures. This concept was imaginatively used

---

Department of Chemistry, University of North Carolina at Chapel Hill, Chapel Hill, NC 27599–3290, USA.

*To whom correspondence should be addressed. E-mail: morken@unc.edu

by Moates *et al.* (5) for the parallel evaluation of the ignition temperatures of 16 spatially addressed metal-doped alumina pellets in the presence of H_2 and O_2 gases at elevated temperature. To date, these approaches have not been realized for the analysis of large (10^4 to 10^6 members) polymer bead–bound libraries for catalysis of typical solution-phase chemical reactions. Whereas 90°C temperature changes on 3 mm by 4 mm solid pellets were observed in the above heterogeneous assay, much smaller temperature changes were expected in solution because of the effective cooling of the 300- to 500-μm polymer beads by reaction solvent. Absorbance of the IR signal by reaction solvent or reagents or both can also pose a complication. Finally, with polymer-bound catalysts, diffusion of reagents through the polymer matrix might limit the reaction rate and result in a leveling effect such that it would not be possible to differentiate catalyst activities over a certain threshold value.

Our preliminary studies centered around the acyl transfer reaction because, until recently, chemists have met with little success in approaching the selectivity of enzymatic acylation catalysts found in nature (6). On the basis of nature's example, multifunctional catalysts that use a concerted interplay between tethered functional groups hold great promise as particularly potent effectors of chemical transformations. The choice of functional groups as well as their relative position and orientation in space are all critical factors for effective rate acceleration. According to proposed mechanisms for various nucleophile catalyzed acylation reactions (Fig. 1) (*7*), we reasoned that a suitable base covalently tethered in the correct orientation relative to a nucleophilic center might increase catalyst activity through a bifunctional catalytic manifold. Additional interactions, for example, those that stabilize the intermediate acylpyridinium salt or that bind to the reacting alcohol, might lead to further increases in reactivity.

To develop a thermographic assay for our envisioned library, we used an IR camera (Cincinnati Electronics IRRIS 256ST, 256 × 256 InSb FPA detector) to examine both noncatalyst beads (acylated 300-μm tentagel S-NH_2; Rapp Polymere) and those with a known acylation catalyst attached (*N*-4-pyridylproline coupled to polymer resin) (8). Although in the reaction solution (8:1:1:1 chloroform:ethanol:acetic anhydride:triethylamine) it was not possible to see individual noncatalyst beads with the IR camera (bead temperature rapidly equilibrates with solvent), catalyst beads exhibited a sustained ∼1°C temperature increase from that of the bulk solvent. This temperature difference is easy to observe with the IR camera (detection limit = 0.02°C; see Fig. 2A), indicating that active catalyst beads can be reliably distinguished from those that are inactive. With chloroform as solvent, the beads rose to the top of the reaction solution, thus avoiding solvent interference with IR transmission. When the proportion of chloroform was reduced such that the beads sank, it was not possible to observe hot beads with the camera.

With a working assay developed, an encoded (9) library was prepared by split and pool solid-phase synthesis (*10*), with the reaction sequence and monomers shown in Fig. 3 (*11*). In addition to a variety of basic groups and a diverse collection of potentially nucleophilic compounds, a subset of library monomers was chosen at random on the chance that they might act through an unpredicted mode of catalysis. Additionally, *N*-4-pyridylproline (**B12**) was included as a control in the second monomer group to ensure that effective catalysts were present. For library synthesis, initial displacement of an activated

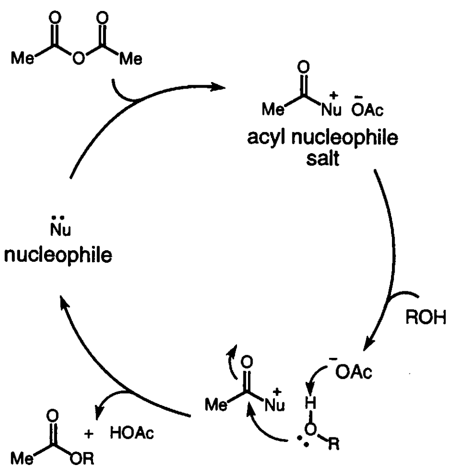

Fig. 1. Mechanism for the nucleophile (Nu) catalyzed reaction between acetic anhydride and alcohols. Ac, acetyl; Me, methyl.

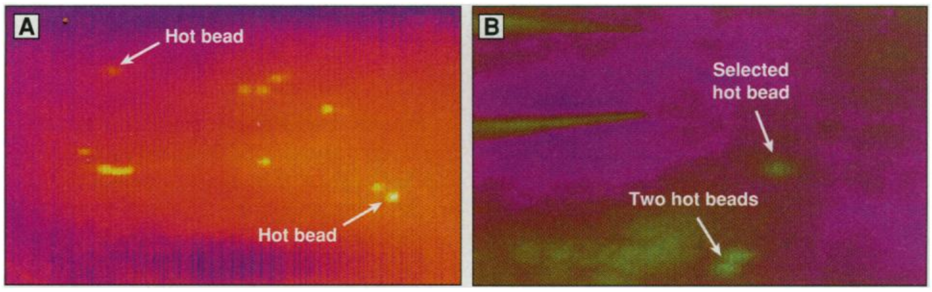

Fig. 2. (**A**) Infrared thermographic image of ∼20 catalyst beads in the presence of ∼3000 noncatalyst beads. Arrows indicate 2 of the 14 visible hot beads. (**B**) Closeup IR thermographic image of the trimeric catalyst library in the presence of acylation reagents, showing one hot bead being selected for decoding (tweezers in upper left).

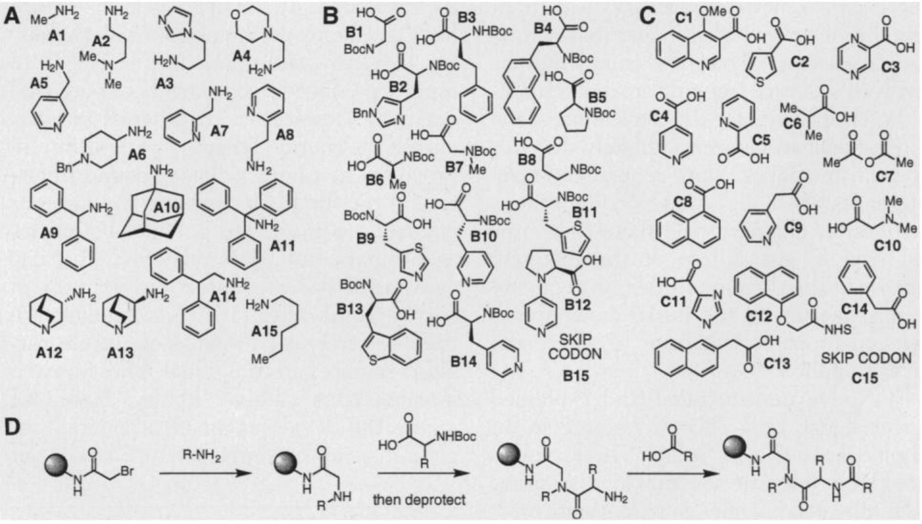

Fig. 3. Synthesis scheme and monomers used in the three positions of the trimeric catalyst library. (**A**) Amine monomers, (**B**) amino acid monomers, (**C**) acid monomers, and (**D**) library synthesis. Boc, butoxycarbonyl; Bn, benzyl.

bromide with a variety of primary amines (**A1** to **A15**) was followed by coupling a variety of protected amino acids (**B1** to **B15**) to the resulting secondary amine nitrogen. After deprotection, a collection of carboxylic acids (**C1** to **C15**) was coupled to the liberated amine terminus, thereby completing the trimeric library. With 15 monomers in each position (including a skip codon) (*12*), the library should be composed of 3150 distinct compounds.

The addition of 610 mg of library resin beads (~7000 beads) to a solution composed of 40 ml of chloroform, 6 ml of ethanol, 6 ml of triethylamine, and 3 ml of acetic anhydride revealed beads with a range of temperatures; however, the bulk maintained temperatures close to background. Appropriate adjustment of the IR camera's temperature display span allowed for visualization of only the hottest beads. Over time, average bead temperature appeared to decrease, presumably because of the consumption of reagents; the addition of fresh reagents increased bead temperature. Of the hottest beads, 23 were selected (Fig. 2B) and subsequently decoded (not all of the hottest beads were selected for decoding). As shown in Table 1, of the 23 selected and decoded beads, 21 were either **1** or **2**, prepared from amines **A12** and **A13**, coupled to acid *N*-4-pyridylproline (**B12**). Attachment of monomer **B12** in the amino acid position effectively terminates compound synthesis because **B12** does not have an amine on which to couple an acid in the third position. In addition to **1** and **2**, beads containing sequences coding for compounds **3** and **4** were also selected.

Table 1. Selection frequency and structures of beads from the IR catalyst library assay. Ph, phenyl.

predicted compound	occurrences	encoding sequence		
		amine	amino acid	acid
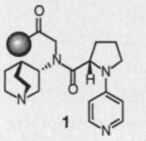 1	11	A12	B12	-
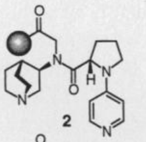 2	10	A13	B12	-
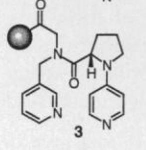 3	1	A5	B12	-
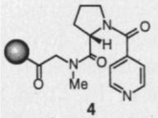 4	1	A1	B5	C4
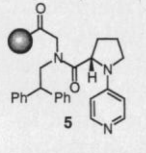 5	0	A14	B12	-

To ascertain whether the assay reflects catalyst activity, we studied compounds of interest with a series of kinetic experiments. After resynthesis on aminomethyl polystyrene macrobeads, five beads of a given catalyst were added to 1.1 ml of an 8:1:1:1 solution of chloroform:acetic anhydride:1-butanol:triethylamine. The average percentage of reaction at 9 min for three kinetic runs is shown in Fig. 4. After subtraction of background reaction (13% at 9 min), noncatalyst beads (*N*-acetate–capped beads, **6**) showed little catalytic activity (~1% conversion after 9 min). Hot beads **1**, **2**, and **3** all gave substantial conversion (39, 24, and 23%, respectively), as compared with the noncatalyst beads and structure **5** (9% conversion), a compound that should have been present in the library but was not selected. Beads containing compound **4** gave no rate acceleration above background, indicating that the wrong bead may have been selected during the assay. When **B12** was attached directly to beads and used in these kinetic runs, 14% conversion was achieved at 9 min. Thus, **A12** appears to enhance the catalytic activity of the *N*-4-pyridylproline nucleus. Although it is peculiar that both **A12** and its enantiomer **A13** were selected from the assay whereas nonracemic L-proline was used for the synthesis of **B12** (*13*), control experiments indicated that, under slow amide-coupling conditions, **B12** is racemized and similar enantiomeric diastereomer mixtures are likely present on both beads **1** and **2**. At this point, no mechanistic conclusions can be drawn in regard to the enhanced activity of **1** relative to polymer-bound *N*-4-pyridylproline.

Table 2. Calculated enthalpy change (ΔH_r°) for selected chemical reactions. ΔH_r° was calculated from thermochemical data reported in (*15*). *t*, tert; Bu, butyl.

Reaction	ΔH_r° (kcal/mol)
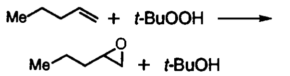	-51.1
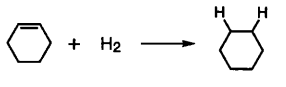	-28.3
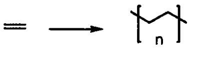	-25.5
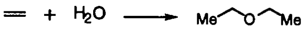	-27.6
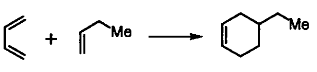	-40.4

Several points in regard to the assay merit mention. Structure **1**, one of the most strongly selected beads (11 beads selected from the ~30 present in the assay), also showed the most efficient catalysis in the kinetic runs as compared with all others. This result indicates that, to a rough approximation, selection frequency reflects catalyst activity and may be used as an indicator of catalyst efficiency (*14*). Statistically, 1 bead in 15 should have **B12** in the second monomer position, and compounds **1** and **2** should each be present once in every 225 beads. Because **B12** is a cap, compounds containing this monomer are present at a frequency 15 times greater than that of any other compound. In the entire 7000 beads screened, ~60 beads should be either compound **1** or **2**. That it was possible to select 21 of these beads to the near exclusion of the other ~400 **B12**-containing beads present highlights the reliability of the assay. Also of note is the extent to which the assay can discriminate between similar levels of activity: Compound **5**, a catalyst with about fourfold less activity than **1**, was present in the library assay (~30 beads) but was not selected.

Although reactions with lower catalyst turnover rates might be more challenging, evaluation of organometallic libraries or libraries of ligands for ligand-accelerated metal catalysis should not require substantial modifications to the above described protocol. Efficient catalysis of the acylation reaction studied here is reported to be exothermic ($\Delta H_r^\circ = -14.9$ kcal/mol) (*15*);

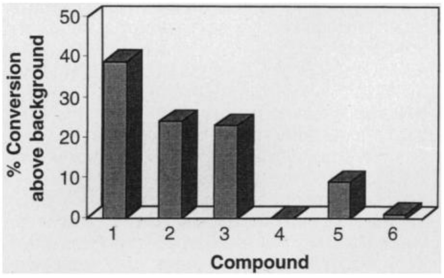

Fig. 4. Percentage of conversion above background (13%) at 9 min for polymer bead–bound compounds. The conditions were as follows: five beads (500 μm polystyrene, 1.04 mmol/g) of a given compound were added to a stirred solution of 1.1 ml of 8:1:1:1 $CHCl_3$:triethylamine:*n*-BuOH:Ac_2O. Conversion was measured by gas chromatography versus zero time sample with an internal standard.

however, it does not involve an atypical enthalpy change, as compared with many reactions of current interest in both academic and industrial synthesis (Table 2). In general, analysis of combinatorial libraries should reveal novel catalyst structures with potentially new modes of catalysis, as observed here.

REFERENCES AND NOTES

1. F. M. Menger, A. V. Eliseev, V. A. Migulin, *J. Org. Chem.* **60**, 6666 (1995).
2. G. Liu and J. A. Ellman, *ibid.*, p. 7712; K. Burgess, H. J. Lim, A. M. Porte, G. Sulikowski, *Angew. Chem. Int. Ed. Engl.* **35**, 220 (1996); B. M. Cole *et al.*, *ibid.*, p. 1668.
3. K. S. Lam *et al.*, *Nature* **354**, 82 (1991); J. K. Chen, W. S. Lane, A. W. Brauer, A. Tanaka, S. L. Schreiber, *J. Am. Chem. Soc.* **115**, 12591 (1993); A. Borchardt and W. C. Still, *ibid.* **116**, 373 (1994); M. T. Burger and W. C. Still, *J. Org. Chem.* **60**, 7382 (1995); M. B. Francis, N. S. Finney, E. N. Jacobsen, *J. Am. Chem. Soc.* **118**, 8983 (1996); H. P. Nestler, H. Wenemers, R. Sherlock, D. L. Y. Dong, *Bioorg. Med. Chem. Lett.* **6**, 1327 (1996).
4. I. P. Nagy and J. A. Pojman, *Chem. Phys. Lett.* **200**, 147 (1992); K. Kustin and E. W. Ross, *J. Chem. Educ.* **70**, 454 (1993); I. Eskendirov, B. Kabongo, L. Glasser, V. D. Sokolovskii, *J. Chem. Soc. Faraday Trans.* **91**, 991 (1995).
5. F. C. Moates *et al.*, *Ind. Eng. Chem. Res.* **35**, 4801 (1996).
6. E. Vedejs and X. Chen, *J. Am. Chem. Soc.* **118**, 1809 (1996); J. C. Ruble and G. C. Fu, *J. Org. Chem.* **61**, 7230 (1996); J. C. Ruble, H. A. Latham, G. C. Fu, *J. Am. Chem. Soc.* **119**, 1492 (1997); T. Kawabata, M. Nagato, K. Takasu, K. Fuji, *ibid.*, p. 3169.
7. A. Fersht and W. P. Jencks, *J. Am. Chem. Soc.* **92**, 5432 (1970); E. Guibe-Jampel, G. Le Corre, M. Wakselman, *Tetrahedron Lett.* 1157 (1979); G. Hofle, W. Steglich, H. Vorbruggen, *Angew. Chem. Int. Ed. Engl.* **17**, 596 (1978); E. Vedejs and S. T. Diver, *J. Am. Chem. Soc.* **115**, 3358 (1993).
8. For relevant studies, see E. J. Delaney, L. E. Wood, I. M. Klotz, *J. Am. Chem. Soc.* **104**, 799 (1982); M. Tomoi, Y. Akada, H. Kakiuchi, *Makromol. Chem. Rapid Commun.* **3**, 537 (1982); F. M. Menger and D. J. McCann, *J. Org. Chem.* **50**, 3928 (1985); A. Deratani, G. D. Darling, D. Horak, J. M. J. Frechet, *Macromolecules* **20**, 767 (1987).
9. M. H. Ohlmeyer *et al.*, *Proc. Natl. Acad. Sci. U.S.A.* **90**, 10922 (1993).
10. A. Furka, F. Sebestyen, M. Asgedom, G. Dibo, *Int. J. Pept. Protein Res.* **37**, 487 (1991).
11. Library synthesis was performed on aminomethyl polystyrene macrobeads (500 μm, 1.04 mmol/g; Rapp Polymere, Tübingen, Germany), because catalysts on this polymer support were found to give a larger temperature increase in a related assay developed in our labs.
12. A. P. Combs *et al.*, *J. Am. Chem. Soc.* **118**, 287 (1996).
13. **B12** was prepared by treatment of L-proline *tert*-butyl ester (2 equiv.) and 4-bromopyridine (1 equiv.) with diisopropylethylamine (3 equiv) in dimethyl sulfoxide at 120°C for 12 hours.
14. Synthesis efficiency or site-site interactions between multiple catalyst moieties may lead to variation in observed activity that does not reflect inherent activity. In regard to catalyst synthesis, preliminary data indicate that the syntheses were successful in the preparation of **1**, **2**, and **5**. Catalyst resynthesis on Rink amide resin (Novabiochem) followed by cleavage from solid support afforded a compound with very clean low-resolution fast atom bombardment mass spectra corresponding to the predicted product in each case. Although these results are not quantitative and are somewhat ambiguous because a different resin was used in resynthesis as compared with library preparation, they do indicate that no fundamental synthesis problems occurred during the preparation of these monomer sequences.
15. J. D. Cox and G. Pilcher, *Thermochemistry of Organic and Organometallic Compounds* (Academic Press, New York, 1970).
16. We thank L. H. Bogart of Cincinnati Electronics (Mason, OH) and R. E. Richardson of Mec-Tric Control (Charlotte, NC) for assistance and use of the Cincinnati Electronics IRRIS-256ST IR camera.

6 October 1997; accepted 23 February 1998

Polyolefin Spheres from Metallocenes Supported on Noninteracting Polystyrene

Stephen B. Roscoe, Jean M. J. Fréchet,* John F. Walzer,
Anthony J. Dias

To obviate the destructive interaction of highly reactive metallocene catalysts with classical silica-based supports while retaining the advantage of supported catalysts, a noninteracting polystyrene support was developed. Supported catalysts for the polymerization of α-olefins are prepared by treating lightly cross-linked, chloromethylated polystyrene beads consecutively with a secondary amine, an ammonium salt of a weakly coordinating anion, and a neutral dialkylmetallocene. Catalytic sites are distributed homogeneously throughout the support particle, and the polymerization occurs within the bead, in contrast to traditional surface-supported metallocene catalysts. The copolymerization of ethylene and 1-hexene at 40°C affords discrete spherical polyolefin beads with a size (0.3 to 1.4 millimeters) that varies according to the polymerization time.

The polymerization of α-olefins by metallocene-based catalysts is at an exciting juncture. Research into a wide variety of cationic metallocene structures, and attendant weakly coordinating anions, has led to the development of families of highly active and selective catalysts, which generate a range of polyolefin products in solution (*1*). However, practical considerations have dictated that industrial olefin polymerizations be performed usually in the heterogeneous mode with supported catalysts. Traditional supports, such as high surface area silica or alumina, have received the most attention and indeed have proven immensely successful in the commercial-scale production of polyolefins. Such acidic supports, however, have reactive surfaces that can lead to catalyst deactivation and thus alternate supports are desirable. We have focused our attention on silica-free supports designed for chemical versatility and rugged physical properties to best exploit state-of-the-art catalysts (*2*). Our approach to designing the support material aims at functionalizing the interior of a swellable but insoluble polymer particle with the appropriate catalyst to allow a nominally heterogeneous polymerization to proceed in a microscopically homogeneous "solution-like" environment. The use of an organic substrate allows us to select a sequence of facile, high-yielding reactions for catalyst preparation (making the procedure well suited for practical uses) or for the combinatorial investigation of α-olefin polymerization. We report here a modular polystyrene (PS)–based support technology that not only yields supported catalysts unusually active at low temperatures but also generates polyethylene-*co*-hexene in the form of discrete, free-flowing, millimeter-sized spheres that grow in proportion to the polymerization time.

The functionalization of polymer resin beads provides an especially suitable method to tailor a heterogeneous catalytic moiety in much the same manner as a homogeneous catalyst. Lessons learned in solution about the design of a catalytic complex may be applied more reliably to a polymer matrix than to the surface of an inorganic support, because an organic material can be designed to more closely resemble the solution environment (*3*). Numerous routes are available for the functionalization of solid resin beads, and a number of polymer-bound catalytic systems have been devised for several important reactions (*4*), including olefin metathesis (*5*) and Ziegler-Natta polymerizations (*6*, *7*). Many of these systems exhibit not only different kinetics, but also different regio- (*8*) and enantio-selectivities (*9*) from their homogeneous and heterogeneous counterparts.

The group IV metallocene catalysts are generated from a neutral precursor complex that is activated by a cocatalyst, such as the combination of a Lewis or Brönsted acid, to abstract a ligand from the metallocene generating a low-valent cation, and a charge-balancing noncoordinating counterion. In many systems described previously, an oligomeric product from the partial hydrolysis of trimethylaluminum (methylalu-

---

S. B. Roscoe and J. M. J. Fréchet, Department of Chemistry, University of California, Berkeley, CA 94720, USA. J. F. Walzer and A. J. Dias, Baytown Polymer Center, Exxon Chemical Company, 5200 Bayway Drive, Baytown, TX 77520, USA.